ACS OMEGA

http://pubs.acs.org/journal/acsodf

Article

Thermosensitive Chitosan-Based Injectable Hydrogel as an Efficient Anticancer Drug Carrier

Anam Ahsan, Muhammad Asim Farooq, and Amna Parveen*

Cite This: *ACS Omega* 2020, 5, 20450−20460

Read Online

ACCESS | Metrics & More | Article Recommendations

ABSTRACT: A thermosensitive, physically cross-linked injectable hydrogel was formulated for the effective and sustained delivery of disulfiram (DSF) to the cancer cells as there is no hydrogel formulation available until now for the delivery of DSF. As we know, hydrogels have an advantage over other drug delivery systems because of their unique properties, so we proposed to formulate an injectable hydrogel system for the sustained delivery of an anticancer drug (DSF) to cancer cells. To investigate the surface morphology, a scanning electron microscope study was carried out, and for thermal stability of hydrogels, TGA (thermogravimetric analysis) and DSC (differential scanning calorimetry) were performed. The rheological behavior of hydrogels was evaluated with the increasing temperature and time. These developed hydrogels possessing excellent biocompatibility could be injected at room temperature following rapid gel formation at body temperature. The swelling index and in vitro drug release studies were performed at different pH (6.8 and 7.4) and temperatures (25 and 37 °C). The cell viability of the blank hydrogel, free DSF solution, and Ch/DSF (chitosan/DSF)-loaded hydrogel was studied by MTT assay on SMMC-7721 cells for 24 and 48 h, which exhibited higher cytotoxicity in a dose-dependent manner in contrast to the free DSF solution. Moreover, the cellular uptake of DSF-loaded hydrogels was observed stronger as compared with free DSF. Hence, chitosan-based hydrogels loaded with DSF possessing exceptional properties can be used as a novel injectable anticancer drug for the sustained delivery of DSF for long-term cancer therapy.

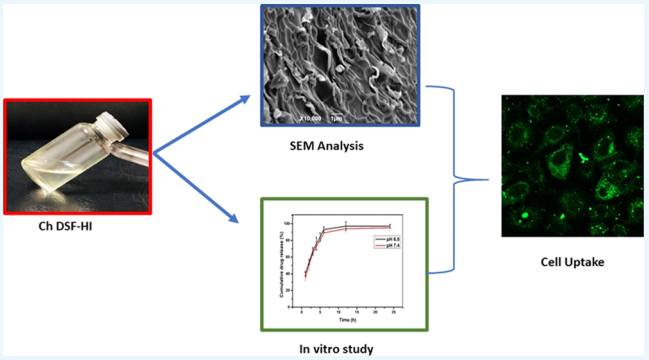

1. INTRODUCTION

Cancer is one of the emerging diseases globally. Chemotherapy is usually employed for the treatment of many cancer types in the world; however, many side effects are associated with chemotherapy and anticancer drugs, which are a major challenge for rational therapy. To address this problem, the development of smart drug delivery systems (DDs) could be useful to sustain the release of the drug into the cancer tissues, with minimal side-effects to healthy tissues.[1,2] Hydrogels are three-dimensional systems constructed by different polymers.[3] Thermoresponsive hydrogels can be promising DDs for the controlled release of the drug at desirable sites.[4] Injectable hydrogels have numerous advantages as compared to other DDs:[5] first, their biocompatibility, easy fabrication, and easy injectability into the tumor sites and second, high drug loading (DL) of anticancer drugs could be achieved by injectable hydrogels.[6] Chitosan (CS) is a derivative of chitin and obtained by the alkaline deacetylation process. It has various properties, such as nontoxicity, biodegradability, and biocompatibility, with multiple applications in different fields such as biomedicine and DDs.[7,8] In recent years, chitosan-based hydrogels have obtained significant consideration for many hydrogel applications because of their excellent material properties.[9,10]

Disulfiram (DSF) has been widely used for the treatment of alcoholism since the 1930s, and it has also been approved by the food and drug administration (FDA).[11] The DSF mechanism of action associated with the treatment of alcoholic disease inhibits aldehyde dehydrogenase (ALDH).[12,13] Numerous mechanisms of DSF anticancer activity have been reported in the literature, including irreversible inhibition of ALDH and P-glycoprotein (P-gp).[14,15] In recent years, DSF has confirmed its cytotoxic effects against various cancers including, lung carcinoma,[16] prostate carcinoma,[17] breast cancer,[13] and colorectal cancer.[18]

Until now, no study has been performed for the fabrication of thermosensitive chitosan-based DSF-loaded injectable

Received: May 29, 2020
Accepted: July 24, 2020
Published: August 10, 2020

hydrogels for the effective and sustained delivery of DSF for cancer therapy. The drug-loaded hydrogel is a mature system for the delivery of various drugs. However, research on disulfiram as an anticancer agent has started in recent years; hence, only few drug DDs are studied so far for the delivery of disulfiram, that is, disulfiram-loaded nanoparticles, micelles, and nanosuspensions. However, no hydrogel system for DSF delivery has been formulated, so our main aim was to develop a chitosan-based hydrogel system that could release DSF in a sustained manner for long-term cancer treatment in an efficient way. The chitosan polymer was used for this purpose because of its easy handling and unique properties. The hydrogel was prepared by the self-assembly method as this is a unique and efficient method[19,20] and evaluated for sol−gel transition behavior, rheological analysis, swelling index (SI) measurement, DL, encapsulation efficiency (EE), *in vitro* drug release test, and *in vitro* erosion test. The hydrogel was also subjected to surface morphology examination through a scanning electron microscope and other physiochemical characterizations, thermogravimetric analysis (TGA), and differential scanning calorimetry (DSC). Human HCC cells (SMMC-7721) were used to determine the therapeutic activity of DSF released from the hydrogel. Moreover, the cellular uptake of the fluorescein isothiocyanate (FITC)-loaded hydrogel was investigated by confocal microscopy and flow cytometry, respectively.

2. RESULTS AND DISCUSSION

2.1. pH Measurements. The pH of the final sol and the gel was checked. The pH of the final sol was 6.93 ± 0.07, while the gel was 7.13 ± 0.06. The pH of the prepared hydrogel was checked in order to ensure that there is no drastic change in pH value after conversion of sol to gel, which could occur because of any undesired chemical reaction in the system. We aimed to deliver the hydrogel at physiological pH for the efficient delivery of the drug, so we monitor the pH of the hydrogel system.

2.2. Visual Transparency of the Hydrogel Injection. Visual evaluation of the hydrogel was performed at different temperatures (i.e., 25−37 °C) for the assessment of transparency. The Ch/DSF hydrogel was transparent at the experimental temperature (25 °C), which proves that the added ingredients are homogeneously mixed.[21] It was observed that the hydrogel became turbid at body temperature in comparison to the initial sol (Figure 1).

2.3. Optical Transparency as a Function of Temperature. To evaluate the Ch/DSF thermosensitive injectable hydrogel, a temperature-dependent evaluation of light transmittance was done. For this purpose, a water bath and UV spectrophotometer were used. As shown in Figure 2, the transmittance was checked at various stages under UV, and the effect of temperature was noted. The hydrogel solution was prepared and shifted into a disposable cuvette. The cuvette was placed in the water bath to notice the changes due to the increase in temperature. It was seen that at low temperature, the hydrogel solution was transparent, but the formulation became cloudy with an increase of temperature above 32 °C, as shown in Figure 1. The reason is that at low temperatures, hydrophilic interaction occurs, keeping the solution uniform and transparent. However, at the higher temperatures, hydrophobic interactions occur, creating the solution milky white and turbid.[22]

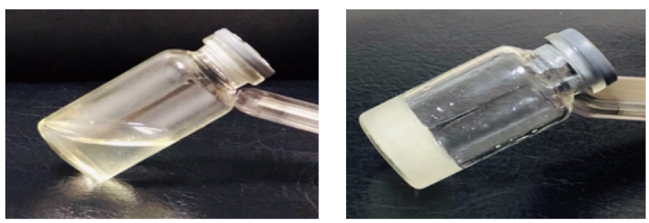

(a) Sol at 25 °C (b) Gel at 37 °C

Figure 1. Phase transition of the hydrogel at room temperature and body temperature.

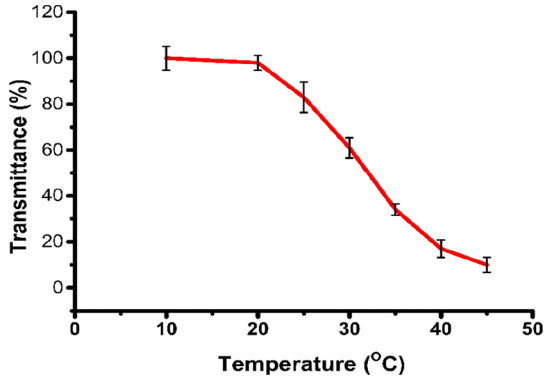

Figure 2. Transmittance of Ch/DSF hydrogel injection as a function of temperature (n = 3).

2.4. Sol−Gel Transition Behavior. To determine the thermal response of the Ch/DSF injectable hydrogel, phase transition studies were performed using the tube invert method. The gelation time and temperature are vital characteristics for the transition of the phase of the thermally responsive hydrogel. Chitosan is a thermally responsive polymer and has been widely used to prepare thermally responsive hydrogels.[23,24] Increasing the concentration of the polymer or drug and other added components has a direct impact on the gelation time and temperature. Hence, by increasing the polymer content, there is an increase in the hydrogen bond formed by the hydrophilic group present in the hydrogel network.[25] The sol−gel transition of the thermoresponsive hydrogel solution took place within a few minutes, that is, 3 min. Figure 1 shows the tube inversion method, where the initial gelation of the hydrogel solution (Ch/DSF) occurred within 3 min. The physicochemical features of the developed formulation are mentioned in Table 1.

2.5. Sol−Gel Fraction. A sol−gel fraction analysis was carried out to evaluate the sol-to-gel ratio of the hydrogels. The study aimed to determine the unreacted polymer concentration in the prepared hydrogel system. The gel fraction in the Ch/DSF hydrogel is more than the blank hydrogel, which may be due to the increased crosslinking between the drug and the polymer. In Ch/DSF thermally responsive hydrogels, it is clear that increasing the concentration of the polymer will lead to an increase in the binding capacity of the system, leading to the decline of the unbound component's amount, thereby forming the gel and *vice versa* (Figure 3).

2.6. Rheological Analysis. The temperature sweep test with a Ch/DSF hydrogel solution between 15 and 60 °C showed a sol−gel transition behavior that occurred at 36.8 °C (Figure 4A). When the temperature increased to 70 °C, the elastic modulus increased to 460 Pa. Both the elastic modulus

https://dx.doi.org/10.1021/acsomega.0c02548
ACS Omega 2020, 5, 20450−20460

Table 1. Physiochemical Features of Ch/DSF-HI

pH					
sol	gel	gelation temperature (°C)	incipient gelation time (s)	DL (%)	EE (%)
6.93 ± 0.07	7.13 ± 0.06	36.8 ± 1.3	180 ± 2	53.17% ± 1.2	93.21% ± 1.3

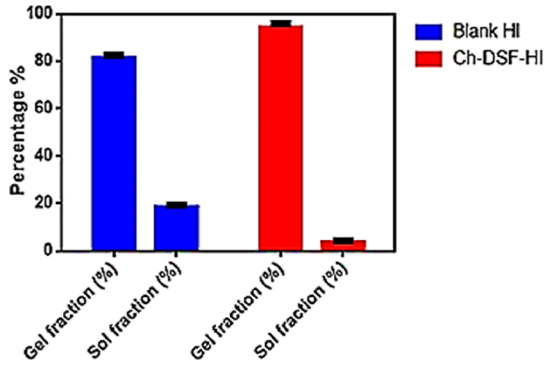

Figure 3. Sol and Gel fraction of blank and Ch/DSF hydrogel injection (n = 3).

(G') and viscous modulus (G'') decreased slightly from 10 °C to almost 30 °C. Then, the elastic modulus began to increase gradually, which confirms the thermosensitive behavior of the hydrogel.[26]

The viscosity of the hydrogel remained higher between 15 and 36 °C and then started to decline till 50 °C. This demonstrates the viscoelastic behavior of the hydrogel as the temperature goes on increasing, that is, more viscous at body temperature than room temperature (Figure 4B). These results are relevant to the previously reported work.[27]

A time sweep test at a temperature of 37 °C for 30 min showed that the elastic modulus (G') gradually increased over time, while the viscous modulus (G'') remained constant. Higher G' demonstrates stronger hydrogel network.[28] This is an indicator of the mechanical reinforcement of the gel in the body temperature over time. It can be seen from Figure 4C that the elastic modulus (G') of the chitosan hydrogel increased from 300 to 669 Pa during a 30 min time scan (n = 3).

2.7. SI Measurement. Swelling is described as a phenomenon in which water/biological fluids are retained in a polymer network. The capability of a hydrogel to swell depends on its chemical structure and the characteristics of its medium.[29] As shown in Figure 5, swelling studies of chitosan-based hydrogels at different temperatures and pH (i.e., at temp 25 & 37 °C and pH 1.2 & 7.4) were performed.

2.7.1. Effect of Temperature on SI. To assess the temperature impact on the swelling behavior of hydrogels, all hydrogels were exposed to a temperature range of 25−37 °C. Figure 5A depicts the swelling behavior of chitosan DSF hydrogels at different temperatures. It can be seen from the graph that an increase in temperature caused an increase in the swelling rate. The reason is that the hydrogen bond of the

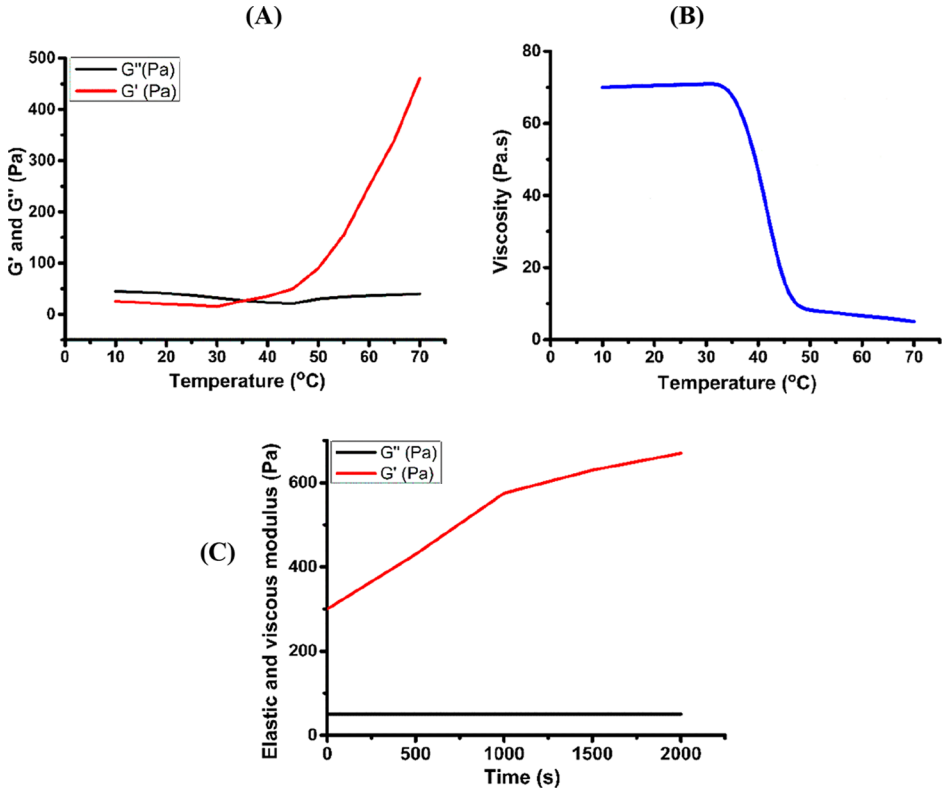

Figure 4. Rheological behavior of hydrogel injection (A) elastic modulus (G') and viscous modulus (G'') of the hydrogel injection as a function of temperature; (B) viscosity (η) of hydrogel injection with the change of temperature; and (C) elastic modulus (G') and viscous modulus (G'') over time.

https://dx.doi.org/10.1021/acsomega.0c02548
ACS Omega 2020, 5, 20450−20460

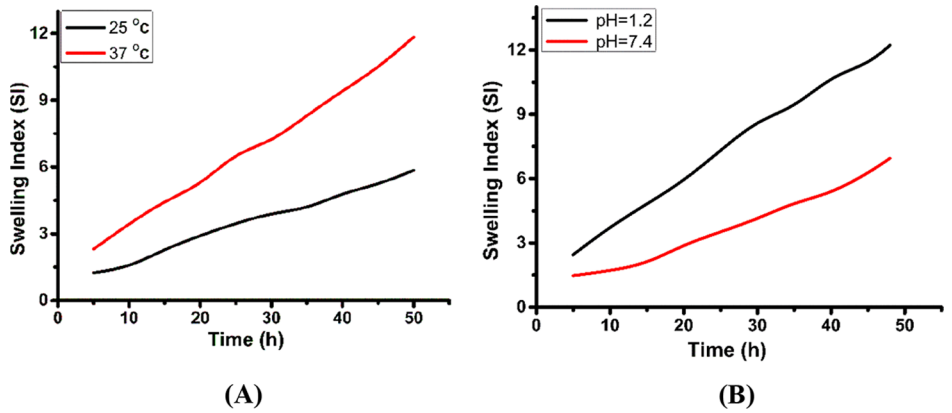

Figure 5. SI measurement of the Ch/DSF hydrogel injection as a function of temperature and time; (A) SI of the hydrogel at different temperatures; (B) SI of the hydrogel at different pH (n = 3).

amine group in chitosan may dissociate with the water molecules inside the hydrogel network. As a result, the polymer chains in the hydrogel relax, which leads to increased swelling.[29] A similar temperature-dependent swelling of the chitosan hydrogel has been described before.[30]

Liu and his colleagues investigated heat-sensitive supramolecular hydrogels, aiming to produce a hydrogel for the efficient and sustained delivery of drugs in response to temperature.[31] Zheng and his team investigated injectable hydrogels with microparticle transitions for tumor targeting in response to temperature change by studying the effect of their hydrogel on K7 osteosarcoma cells in mice.[32]

2.7.2. Effect of pH on SI. Buffer solutions were prepared at pH 1.2 and 7.4 to assess the impact of different pH on the hydrogel swelling behavior. The results showed that the swelling of the hydrogel at 1.2 is higher than that at 7.4 (Figure 5B).

Under acidic conditions, the chitosan hydrogel reached maximum swelling and decreased with increasing pH of its medium (Figure 5B). This is because the concentration of H^+ is higher at low pH values, which increased the ability of the amine group to protonate to chitosan, thereby forming $-NH3^+$. As a result, the polymer chains in the hydrogel dissociated from each other. Conversely, by increasing the pH, the amine groups were deprotonated; hence, the repulsion between polymer chains in the hydrogel was reduced. This led to the rigid structure of the hydrogel and reduced its absorption capacity,[33−35] a process which has been described by Hyunmin.[36] Research carried out by Peter John Dowding[37] showed a similar result. Zhang et al. reported hydrogel injections for the treatment of osteosarcoma. They studied pH-responsive nanogels for the delivery of doxorubicin using hyaluronic acid and cisplatin.[38] Zhang and colleagues investigated the formation of pH-responsive hydrogels that can be used for the synergistic delivery of anticancer drugs.[39]

2.8. Drug Loading (DL %) and Encapsulation Efficiency (EE %). The DL capacity of DSF in the chitosan hydrogel network was excellent. The DSF content in the hydrogel network was about 53.17% ± 1.2, and EE % was 93.21% ± 1.3 (Table 1). DL and EE are higher than previously reported similar hydrogel systems.[40−43]

2.9. *In Vitro* Drug Release Analysis. The cumulative release of DSF from the Ch/DSF hydrogel in vitro was measured by the dialysis membrane method in PBS (pH 6.8 & 7.4) at 37 °C for 24 h.[44] Approximately, 40% of DSF was released in the first hour at pH 6.8, while 35% at pH 7.4. After that, the release was slightly enhanced, reaching 97 and 95% drug release at pH 6.8 and 7.4, respectively (Figure 6). DSF

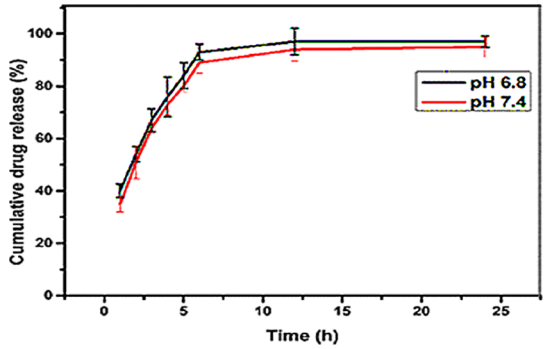

Figure 6. Cumulative drug release (%) from Ch/DSF hydrogel injection overtime at different pH (i.e., pH 6.8, pH 7.4) (n = 3).

release from the Ch/DSF hydrogel followed a biphasic mode, with initial burst release and then continuous release for 24 h at both pH values. Similar results have been shown by Cho et al.[45]

Owing to blocking or absorption by the dialysis membrane bag, 100% of the drug could not be released from the Ch/DSF hydrogel. The initial sudden DSF release from the hydrogel might be due to weak absorption of the drug in the hydrogel network or the quicker dispersion of DSF into the medium or both. Another reason for the initial fast release of the drug from the hydrogel is due to larger pore size of the hydrogel mesh than the size of disulfiram, so the release of drug could be further controlled in future experiments by using a crosslinker to enhance the cross-linking of the hydrogel network.[46] Constant release corresponds to the release of DSF from the compact hydrogel network because of enhanced cross-linking. These results are due to the osmotic pressure difference between the Ch/DSF hydrogel and the released medium. As there is no covalent cross-linking in the Ch/DSF hydrogel to encapsulate DSF, the release of DSF from the hydrogel is by the simple diffusion mechanism.

2.10. *In Vitro* Erosion Test. The chitosan hydrogel was incubated in PBS at 37 °C to study its erosion. Figure 7 presents a curve of the weight change of these hydrogels over time. Hydrogels gradually showed weight loss over three weeks. The slow degradation rate of the hydrogel may be

https://dx.doi.org/10.1021/acsomega.0c02548
ACS Omega 2020, 5, 20450−20460

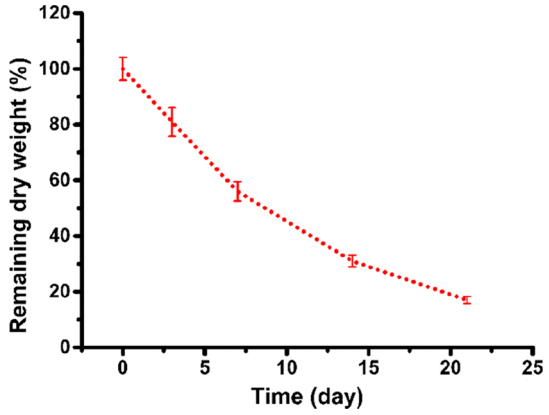

Figure 7. Ch/DSF hydrogel injection degradation study over time (n = 3).

attributed to substantial cross-linking of the hydrogel structure, which imparts strength to the hydrogel, and hence, the degradation rate is slow. The similar erosion profiles of chitosan-based hydrogels have been investigated by various researchers.[28]

2.11. SEM Analysis. SEM investigated the surface morphology of the Ch/DSF hydrogel. Under different cross-sectional and magnification studies, cross-linked hydrogels exhibited a dense and porous network structure (Figure 8).

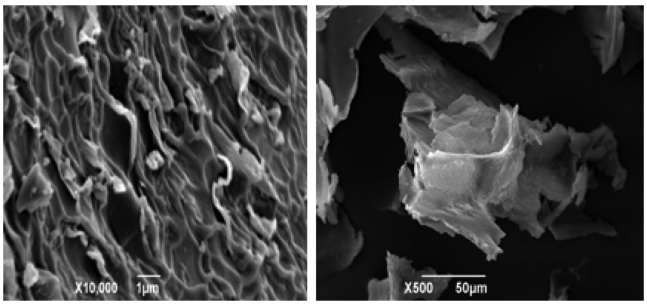

Figure 8. SEM micrographs of Ch/DSF hydrogel injection at different magnification and cross section.

The pores in the hydrogel are due to the existence of DSF in the fabric. This indicates that the interaction between the drug and the polymer is more significant, resulting in the formation of an expanded structure from this cross-linking. This shows the formation of a more stable hydrogel, as reported by previous studies.[47,48]

2.12. TGA and DSC. TGA and DSC characterization were performed for the assessment of the thermal stability of Ch/DSF cross-linked hydrogels. Chitosan degrades at high temperatures.[49] In Figure 9, the initial weight loss of the Ch/DSF hydrogel occurred at 125 °C, which is 10−15%, because of the presence of absorbed water in the hydrogel network. When the temperature increased to 490 °C, further weight loss occurred, while complete degradation of the Ch/DSF hydrogel structure occurred at 800 °C.[50] This degradation at high temperatures indicated that the hydrogel is extensively cross-linked and highly stable over a wide temperature range. As most of the time-release process has to be carried out at a physiological temperature, and our result showed that hydrogel is stable in a physiological temperature range and is also supported by other researchers.[51]

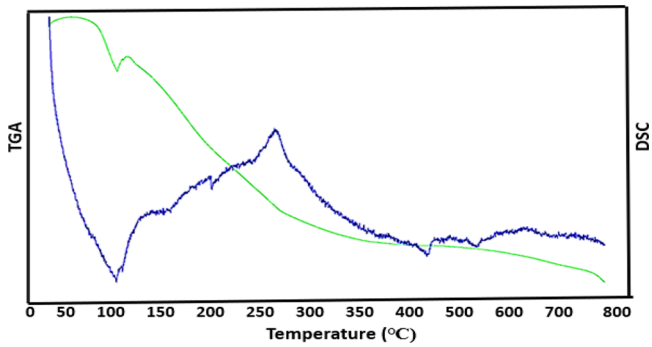

Figure 9. TGA and DSC thermograph of Ch/DSF hydrogel injection.

The DSC curve of the Ch/DSF hydrogel (Ch/DSF-H) is depicted in Figure 9. Because of dehydration of the hydrogel network, the thermogram of Ch/DSF-H displayed an endothermic peak at 125 °C, following an exothermic peak at a range of 550−650 °C, indicating the degradation of the Ch/DSF hydrogel.[52] It is exhibited from the DSC curve that the hydrogel is stable.

2.13. Cytotoxicity Study. At first, the cytotoxicity of the blank hydrogel was evaluated on SMMC-7721 cells. Cells were hatched at 37 °C overnight at various concentrations (0−400 μg mL^{-1}). The cell viability was over 90%, even at 400 μg mL^{-1} (Figure 10A). This low cytotoxicity was suggesting that chitosan has exceptional biocompatibility and safety profile. The low toxicity of chitosan has also been reported in the literature, and many researchers have employed it for the synthesis of implants and injectable hydrogels.[53,54] After overnight incubation, the concentration of DSF and the Ch/DSF hydrogel increased from 0 to 100 μg/mL, and the viability of cells of SMMC-7721 decreased (Figure 10B,C).

Results attained from MTT assay of SMMC-7721 cells at 50 μg mL^{-1} DSF and Ch/DSF hydrogel equivalent conc. showed that the DSF and Ch/DSF-H solution showed 31 and 23% cell viability against SMMC-7721 cells at 24 h. The cell viability further decreased after 48 h of incubation than at 24 h incubation. Besides, these results confirmed that Ch/DSF hydrogel showed a dose-dependent cell proliferation inhibitory effect on SMMC-7721 cells. Notably, at higher drug concentrations, cell viability was decreased by Ch/DSF-H compared to free DSF solutions, suggesting that Ch/DSF-H has higher cytotoxicity. At the same time, DSF in the drug solution is quickly degraded in the cell culture medium, and the higher toxicity of Ch/DSF-H may be attributed to its protective effect on reactive molecules in the cell culture medium and cytoplasm.[55] The lesser free DSF cytotoxicity is also due to the poor water solubility of the drug. Conclusively, the sustained release behavior of DSF from the hydrogel may be the reason for better cytotoxicity inside the cell.[56] Our cytotoxicity study results in the present research are better than the previously reported work. In various studies, the drug and polymer complexes significantly reduced the disadvantageous cytotoxicity of the antitumor drug and polymer complexes as the pharmacokinetic parameters of DDs control the fate of such drugs and polymer complexes.

2.14. *In Vitro* Cell Uptake Study. *2.14.1. CLSM Analysis.* For qualitative cellular uptake of free DSF and FITC Ch/DSF-HI in SMMC-7721 cells, CLSM was used based on stronger green fluorescence of drugs. As revealed in Figure 11, stronger green fluorescence was observed by FITC Ch/DSF hydrogel

https://dx.doi.org/10.1021/acsomega.0c02548
ACS Omega 2020, 5, 20450−20460

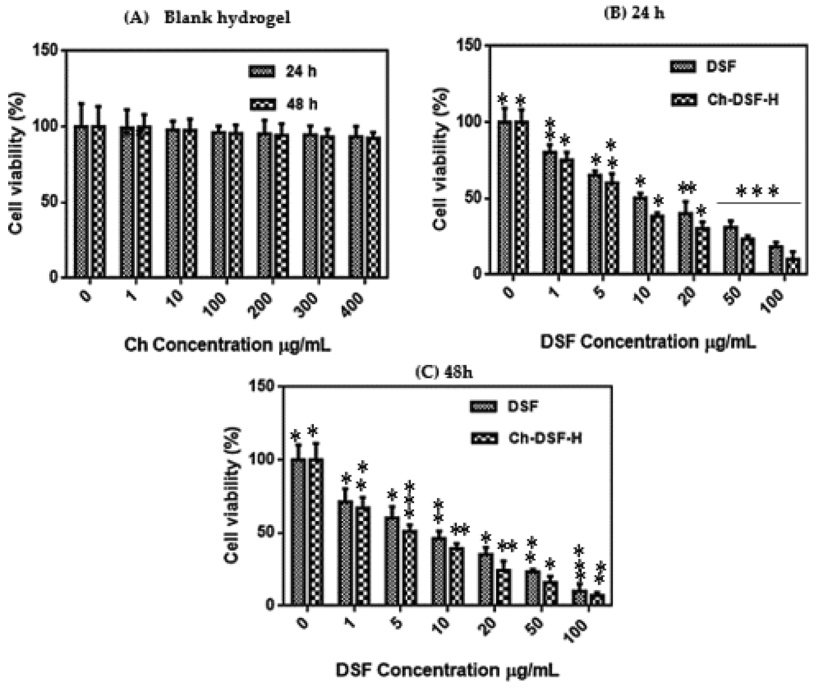

Figure 10. Cell viability of the blank chitosan hydrogel after incubation with SMMC-7721 cells for 24 and 48 h (A), Cell viability of free DSF and Ch/DSF-hydrogel injection (Ch/DSF-H) after incubation with SMMC-7721 cells for 24 h (B) and 48 h (C) respectively. Values represent mean ± SD (n = 3). All experiment performed in triplicates. *p < 0.05, **p < 0.01 and ***p < 0.001, unpaired Student's t-test.

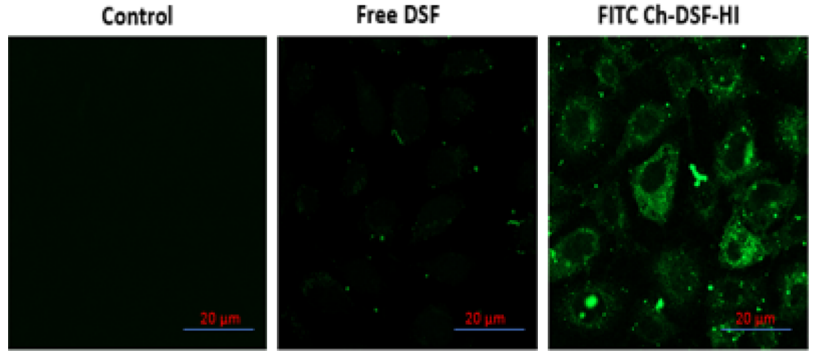

Figure 11. Cellular uptake of free DSF and FITC Ch DSF-HI in SMMC-7721 cells after 4 h incubation; scale bar: (20 μm).

injection (Ch/DSF-HI) in contrast to the free DSF in SMMC-7721 cells. This result indicates that the drug-loaded hydrogel can quickly enter into the cells after 4 h incubation.

2.14.2. Flow Cytometry. For quantitative cell uptake and providing more evidence, flow cytometry was used to explore the cellular uptake of free DSF and FITC Ch/DSF-HI in SMMC-7721 cells for 4 h. The results (Figure 12) showed that FITC Ch/DSF-HI exhibited higher mean fluorescence intensity as compared with free DSF, which further confirms that the drug-loaded hydrogel is taken up to a greater extent by the cells. These results were consistent with the result of CLSM.

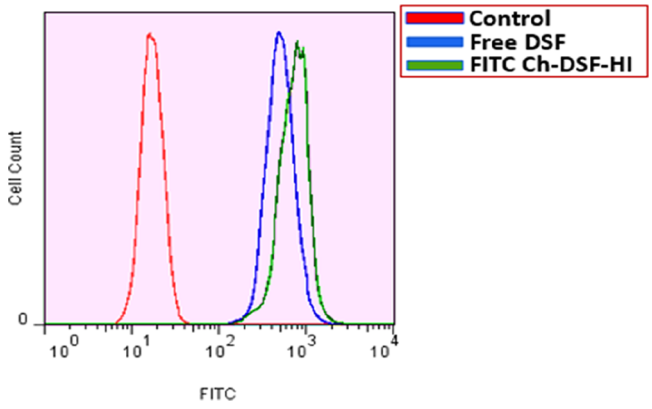

Figure 12. Flow cytometry image of SMMC-7721 cells treated with free DSF and FITC Ch/DSF-HI for 4 h.

3. CONCLUSIONS

Novel injectable thermosensitive hydrogels were developed by the sol−gel methodology, and further, its formulation was confirmed by characterization tests. The developed hydrogel displayed sustained delivery of DSF over time. The swelling studies exhibited that hydrogels showed maximum swelling at 37 °C and pH 1.2 while less swelling at temperature 25 °C and pH 7.4, confirming the efficient delivery of DSF at physiological conditions. Rheological studies proved the dynamic viscoelastic behavior of the injectable hydrogel over

https://dx.doi.org/10.1021/acsomega.0c02548
ACS Omega 2020, 5, 20450−20460

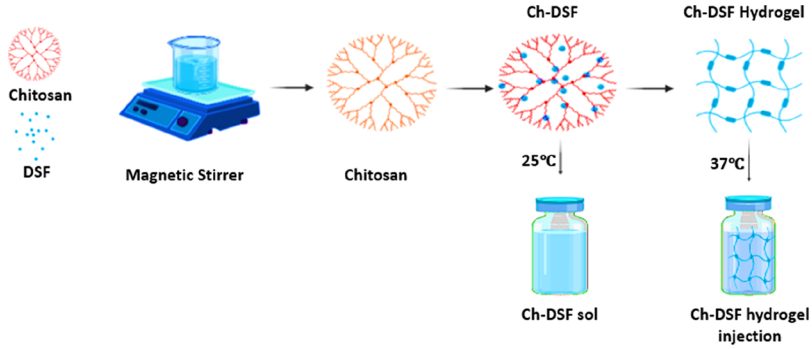

Figure 13. Schematic illustration of the thermosensitive Ch/DSF hydrogel formulation.

temperature and time sweep with incipient temperature 36.8 °C. The hydrogel also exhibited an excellent *in vitro* drug release and erosion profiles.

Cell cytotoxicity of the blank chitosan hydrogel indicates the excellent safety profile, and the Ch/DSF hydrogel showed more toxic effects as compared with free DSF solution in a dose-dependent manner against human HCC cell lines SMMC-7721 cells at 24 and 48 h. Moreover, CLSM and flow cytometry results were consistent with each other and showed higher cell uptake by formulation as compared with the free DSF solution. Hence, it can be concluded that the formulated hydrogel injection could be proposed for the efficient and sustained delivery of DSF for cancer treatment after further investigations.

4. EXPERIMENTAL SECTION

4.1. Materials. Chitosan (average viscosity 5,270,000 Da and DD 86%), disulfiram (99% purity), and MTT reagents were purchased from Sigma-Aldrich, USA. The human HCC cell line SMMC-7721 was purchased from the Chinese Academy of Sciences cell bank, Shanghai, China. Fetal bovine serum (FBS), RPMI 1640, and trypsin were purchased from Thermo Fisher Scientific, Inc. (USA). Glycerol was purchased from Merck, Germany. FITC was purchased from Solarbio Science and Technology Co., Ltd. (Beijing, China). The dialysis membrane (3.5 kDa) was obtained from Shanghai Gene Ray Biotech Co., Ltd. Shanghai, China. All other reagents used in the experiment were of analytical grade.

4.2. Methods. *4.2.1. Preparation of the Chitosan/Disulfiram (Ch/DSF) Hydrogel.* The hydrogel was formulated by dissolving 2 g of chitosan in lactic acid (1%) solution and 1.5 mL of glycerol in distilled water under continuous moderate stirring on a magnetic stirrer for 2 h to get a homogenized hydrogel. Finally, the drug (disulfiram) (2 mg) was added to the chitosan hydrogel under continuous stirring until the drug completely gets dispersed in the gel. Place the gel in an ultrasonic bath for further 30 min to eradicate entrapped air bubbles.[57] A schematic illustration for the gelation process of the Ch/DSF hydrogel is presented in Figure 13.

4.2.2. pH Measurements. The pH of the hydrogel injection was measured by using a digital pH meter. All measurements were done in a triplicate manner.

4.2.3. Visual Transparency of the Hydrogel Injection. Transparency of the formulated hydrogel injection was determined at different temperatures, that is, 25−37 °C. At all temperatures, a transparent solution proves that all the added ingredients are homogeneously mixed.

4.2.4. Optical Transparency as a Function of Temperature. The optical transparency of the prepared hydrogel was analyzed by a UV spectrophotometer at λ 450 nm with varying temperatures. 100% transmittance was defined as the transmission of light passed through distilled water. The sample was placed in the cuvette and kept in a digital water bath with slowly increasing the temperature from 25 to 37 °C. The sample was kept at a particular temperature for almost 5 min and then analyzed by a UV spectrophotometer.[22]

4.2.5. Sol−Gel Transition Behavior. 4.2.5.1. Gelation Temperature. The gelation temperature was assessed by heating the Ch/DSF solution in a glass vial with mild shaking until it is converted to gel. The glass vial was inverted after specific intervals to check gelation. When the solution stopped flowing on tilting the vial, that point was accounted as the gelation temperature.

4.2.5.2. Gelation Time. The gelation time was assessed by the test-tube inverted method. In this method, the freshly prepared Ch/DSF solution (3 mL) was taken in a glass vial and heated in a water bath at 37 °C with gentle shaking, allowing its gelation. After every one min, the glass vial was taken out and inverted at 90° angle for 1 min to check the gelation of the sample. The incipient gelation time was termed as when the solution stopped flowing.

4.2.6. Sol−Gel Fraction. Sol−gel fraction examination was carried out for the determination of the sol and gel fraction in the prepared Ch/DSF thermosensitive hydrogel. The liquid portion of the hydrogel is expressed as the sol fraction. For carrying out this study, discs of dried hydrogel were weighed and kept in boiling water at 100 °C for approximately 4 h. The discs were removed from the water bath after 4 h and dried at room temperature for 24 h. Subsequently, they were placed in the incubator at 37 °C.[58] For calculating the sol and gel fraction of the hydrogel, the following formula was employed

$$\text{gel fraction } \% = W_a/W_b \times 100 \quad (1)$$

$$\text{sol fraction } \% = 100\text{-gel fraction} \quad (2)$$

where W_a is the dry weight of the hydrogel, whereas W_b represents the weight of the hydrogel after extraction for a definite time, that is, 4 h.

4.2.7. Rheological Analysis. The rheology measurement of the hydrogel was performed using a rheometer (TA Instruments, TA-AR 2000, Newcastle, DE, USA) with a conical geometry (Ø = 40 mm, 2°). During heating at a temperature of 15−37 °C, the changes in storage (G') and loss modulus (G'') were recorded at a constant frequency of 1 Hz during the oscillation measurement. Also, the temperature was maintained at 37 °C for 30 min to notice the change in the viscoelastic

https://dx.doi.org/10.1021/acsomega.0c02548
ACS Omega 2020, 5, 20450−20460

behavior of the hydrogel over time. When the material begins to show more viscosity than elasticity (sol−gel transition), the incipient gel point of the solution was evaluated by the intersection of G' and G'' ($\tan \delta$: $G''/G' = 1$).[59]

4.2.8. SI Measurement. Hydrogel swelling experiments were performed using buffered solutions of pH 1.2 and 7.4 at 25 and 37 °C, respectively. Dry hydrogels were accurately weighed. The dry hydrogel samples were swelled in PBS (pH 1.2 and 7.4) at 25 and 37 °C, respectively, while shaking on a horizontal shaker to attain their particular swelling equilibrium. After removing excess surface water with a filter paper, we measured the weight of the swollen gel and calculated its SI by the following formula

$$\mathrm{SI} = (W_s - W_d)/W_d \quad (3)$$

where W_s = weight of the swollen hydrogel, and W_d = weight of the dry hydrogel.

4.2.9. DL and EE. Drug loading (DL %) and encapsulation efficiency (EE %) of Ch/DSF-H were determined by thoroughly crushing the hydrogels in a sterile pestle and mortar. The weighed quantity of the powdered hydrogels was placed in 500 mL of PBS for 24 h under continuous stirring at 37 °C. Subsequently, it was centrifuge it at 3000 rpm. The supernatant was separated by a pipette, filtered by 0.45 μm filter paper, and analyzed for DSF through a UV spectrophotometer at λ_{max} 275 nm.[60] The DL % and EE % were calculated by the following equations:

$$\mathrm{DL}\ \% = \text{amount of DSF in hydrogel/weight of hydrogel} \times 100 \quad (4)$$

$$\mathrm{EE}\ \% = \%\ \text{actual loading/}\%\ \text{theoretical loading} \times 100 \quad (5)$$

4.2.10. In Vitro Drug Release Test. The dialysis membrane method was employed to evaluate the drug release behavior of DSF from the lyophilized hydrogel. Then, 2 mg of lyophilized hydrogels was placed in 5 mL of PBS (pH = 6.8 and 7.4) and shifted to the dialysis membrane bag (MWCO 3.5 kDa). Both ends of the dialysis bag were tightly fastened and immersed in the beakers containing 500 mL of PBS 6.8 and PBS 7.4 pH, respectively.

The release medium was stored at 37 ± 1 °C for 24 h at a shaking speed of 100 rpm. At specific time intervals (1, 2, 3, 4, 5, 6, 12, and 24 h), we took 3 mL of aliquot from the outside of the dialysis membrane and replaced it with the same volume of freshly prepared PBS throughout the experiment. The amount of DSF released from the hydrogel was determined by a UV spectrophotometer at λ_{max} 275 nm. The following formula was used to calculate the cumulative release percentage of DSF from Ch/DSF-H

$$\text{cumulative drug release}\ (\%) = \text{DSF released/DSF loaded} \times 100 \quad (6)$$

4.2.11. In Vitro Erosion Test. To estimate the weight loss by hydrolytic degradation over time, the hydrogels were divided into four groups (3, 7, 14, and 21 days). Each hydrogel was prepared by mixing 2 mL of chitosan/DSF mixture in a 15 mL tube at 37 °C. Then, 10 mL of PBS was added over these prepared hydrogels at 37 °C. After regular time intervals, samples were removed from the solution, blotted dry, and then weighed to calculate the weight (W_t) of the remaining mass. The PBS was changed every three days, and the experiment was performed in triplicates. The following formula calculated the remaining weight % of the hydrogel

$$\text{remaining weight percent}\ (\%) = (W_t/W_o) \times 100 \quad (7)$$

where W_o = initial weight of the dry hydrogel, and W_t = weight of the dry hydrogel after immersion in PBS for different time intervals.

4.2.12. SEM Analysis. For analyzing the internal microstructure of the hydrogels, scanning electron microscopy was performed. The prepared Ch/DSF hydrogel was frozen below −80 °C for 48 h following lyophilization for 24 h. The lyophilized sample was splintered in liquid nitrogen to attain the cross section. It was gold-coated by a sputter coater ((Emitech K575) and then observed by scanning electron microscopy (JSM-5600, Tokyo, Japan), under 20 mA current and an accelerating voltage of 10 kV.

4.2.13. Thermogravimetric Analysis. The resulting hydrogel was subjected to TGA analysis to begin a range of degradation temperatures. Samples for TGA analysis were prepared by crushing the resulting hydrogel, connecting an open pan (100 μL of platinum) to a microbalance, and placing 0.5−5 mg of sample in it. All samples were heated at a rate of 20 °C/min from 25 to 500 °C in a ramp-up test type in dry nitrogen under a standard mode. All measurements were repeated three times.

4.2.14. Differential Scanning Calorimetry. DSC was used to assess the thermal stability of the hydrogel. DSC studies were performed using a DSC device (DSC Diamond Series, Perkin Elmer, USA). The sample was dried with an aluminum pan under a stream of nitrogen at a rate of 40 °C/min.

4.2.15. Cytotoxicity Study. 3-(4,5-Dimethyl thiazolyl-2)-2,5-diphenyltetrazole bromide (MTT) analysis was employed for the assessment of *in vitro* cell viability of the blank hydrogel, plain DSF solution, and Ch/DSF hydrogel (Ch/DSF-H). A 96-well culture plate was used for seeding of cells at a concentration of 4×10^4 cells/well and kept for incubation for 24 h. After that, the cell culture medium was discarded in the 96-well culture plate and substituted with a fresh medium having different concentrations of the blank hydrogel, plain DSF solution, and Ch/DSF-H at 37 °C for 24 and 48 h. After selected time intervals, 20 μL of MTT reagent (5 mg/mL in PBS) was added to each well, and the cells were incubated at 37 °C for 4 h more in the dark. Then, after the medium was removed entirely, DMSO was inoculated to each well and gently stirred to dissolve the formazan dark blue crystals produced by the living cells. The cells without treatment were taken as controls throughout the experiment. Finally, the absorbance was measured on a microplate reader (ELx808; Gene Co., Ltd., Hong Kong, China) at 490 nm.

4.2.16. In Vitro Cellular Uptake Study. The cellular uptake study of free DSF and FITC/Ch/DSF-HI was evaluated by combining the confocal laser scanning microscope (CLSM) and flow cytometry.

4.2.16.1. CLSM Analysis. SMMC-7721 cells were seeded into glass coverslips of 6-well plates at a concentration of 4×10^4 cells/well and cultured at 37 °C for 24 h in a CO_2 5% dampened atmosphere. Then, the cells were incubated with free DSF solution and FITC-tagged Ch/DSF-HI (FITC concentration of 30 μg/mL) at 37 °C for 4 h. Then, the medium was cast off; the cells were washed 3× with PBS and fixed for 10 min, with 4% paraformaldehyde. Finally, the images of the cells were taken by CLSM (CLSM, LSM800,

https://dx.doi.org/10.1021/acsomega.0c02548
ACS Omega 2020, 5, 20450−20460

Germany) with excitation and an emission wavelength at 488 and 522 nm, respectively.

4.2.16.2. Flow Cytometry Analysis. For flow cytometry, after incubation with free DSF and FITC-Ch/DSF-HI (FITC concentration of 30 μg/mL) at 37 °C for 4 h, the cells were collected, washed 3× with PBS, then resuspended in PBS and trypsinized, and centrifuged at 2000 rpm for 15 min. Next, mean fluorescence intensity was measured by FACS Caliber, BD, USA with an excitation wavelength of 488 nm and an emission wavelength of 522 nm selecting the FL-1 channel.

4.2.17. Statistical Analysis. All experimental results were performed thrice, and data are presented as mean ± standard deviation. Statistical significance was evaluated by (ANOVA), and all the analyses were done in comparison with the control group and shown as $***P < 0.001$.

AUTHOR INFORMATION

Corresponding Author

Amna Parveen − *College of Pharmacy, Gachon University, Incheon 406-799, Republic of Korea;* orcid.org/0000-0002-4569-2317; Phone: +82-10-5925-2733; Email: amnaparvin@gmail.com

Authors

Anam Ahsan − *College of Animal Science & Veterinary Medicine, Shanxi Agricultural University, Taigu 030801, PR China*

Muhammad Asim Farooq − *Department of Pharmaceutics, School of Pharmacy, China Pharmaceutical University, Nanjing, Jiangsu 211198, PR China*

Complete contact information is available at: https://pubs.acs.org/10.1021/acsomega.0c02548

Notes

The authors declare no competing financial interest.

ACKNOWLEDGMENTS

This research was supported by the Basic Science Research Program through the National Research Foundation of Korea (NRF) funded by the Ministry of Education (NRF-2019R1G1A1003693).

REFERENCES

(1) Abdelaziz, H. M.; Gaber, M.; Abd-Elwakil, M. M.; Mabrouk, M. T.; Elgohary, M. M.; Kamel, N. M.; Kabary, D. M.; Freag, M. S.; Samaha, M. W.; Mortada, S. M.; Elkhodairy, K. A.; Fang, J.-Y.; Elzoghby, A. O. Inhalable particulate drug delivery systems for lung cancer therapy: Nanoparticles, microparticles, nanocomposites and nanoaggregates. *J. Controlled Release* **2018**, *269*, 374−392.

(2) Gao, S.; Tang, G.; Hua, D.; Xiong, R.; Han, J.; Jiang, S.; Zhang, Q.; Huang, C. Stimuli-responsive bio-based polymeric systems and their applications. *J. Mater. Chem. B* **2019**, *7*, 709−729.

(3) Ahsan, A.; Tian, W.-X.; Farooq, M. A.; Khan, D. H. An overview of hydrogels and their role in transdermal drug delivery. *Int. J. Polym. Mater. Polym. Biomater.* **2020**, 1−11.

(4) Deng, Z.; Guo, Y.; Zhao, X.; Ma, P. X.; Guo, B. Multifunctional stimuli-responsive hydrogels with self-healing, high conductivity, and rapid recovery through host−guest interactions. *Chem. Mater.* **2018**, *30*, 1729−1742.

(5) Li, Y.; Rodrigues, J.; Tomás, H. Injectable and biodegradable hydrogels: gelation, biodegradation and biomedical applications. *Chem. Soc. Rev.* **2012**, *41*, 2193−2221.

(6) Zheng, Y.; Wang, W.; Zhao, J.; Wu, C.; Ye, C.; Huang, M.; Wang, S. Preparation of injectable temperature-sensitive chitosan-based hydrogel for combined hyperthermia and chemotherapy of colon cancer. *Carbohydr. Polym.* **2019**, *222*, 115039.

(7) Omidi, S.; Pirhayati, M.; Kakanejadifard, A. Co-delivery of doxorubicin and curcumin by a pH-sensitive, injectable, and in situ hydrogel composed of chitosan, graphene, and cellulose nanowhisker. *Carbohydr. Polym.* **2020**, *231*, 115745.

(8) Silva, S. S.; Mano, J. F.; Reis, R. L. Ionic liquids in the processing and chemical modification of chitin and chitosan for biomedical applications. *Green Chem.* **2017**, *19*, 1208−1220.

(9) Bhattarai, N.; Gunn, J.; Zhang, M. Chitosan-based hydrogels for controlled, localized drug delivery. *Adv. Drug Delivery Rev.* **2010**, *62*, 83−99.

(10) Kumar, M. N. V. R. A review of chitin and chitosan applications. *React. Funct. Polym.* **2000**, *46*, 1−27.

(11) Farooq, M. A.; Aquib, M.; Khan, D. H.; Hussain, Z.; Ahsan, A.; Baig, M. M.; Wande, D. P.; Ahmad, M. M.; Ahsan, H. M.; Jiajie, J.; Wang, B. Recent advances in the delivery of disulfiram: a critical analysis of promising approaches to improve its pharmacokinetic profile and anticancer efficacy. *Daru, J. Pharm. Sci.* **2019**, *27*, 853−862.

(12) Johansson, B. A review of the pharmacokinetics and pharmacodynamics of disulfiram and its metabolites. *Acta Psychiatr. Scand.* **1992**, *86*, 15−26.

(13) Chen, D.; Cui, Q. C.; Yang, H.; Dou, Q. P. Disulfiram, a clinically used anti-alcoholism drug and copper-binding agent, induces apoptotic cell death in breast cancer cultures and xenografts via inhibition of the proteasome activity. *Cancer Res.* **2006**, *66*, 10425−10433.

(14) Li, H.; Liu, B.; Ao, H.; Fu, J.; Wang, Y.; Feng, Y.; Guo, Y.; Wang, X. Soybean lecithin stabilizes disulfiram nanosuspensions with a high drug-loading content: remarkably improved antitumor efficacy. *J. Nanobiotechnol.* **2020**, *18*, 1−11.

(15) Cvek, B. Targeting malignancies with disulfiram (Antabuse): multidrug resistance, angiogenesis, and proteasome. *Curr. Cancer Drug Targets* **2011**, *11*, 332−337.

(16) Duan, L.; Shen, H.; Zhao, G.; Yang, R.; Cai, X.; Zhang, L.; Jin, C.; Huang, Y. Inhibitory effect of Disulfiram/copper complex on non-small cell lung cancer cells. *Biochem. Biophys. Res. Commun.* **2014**, *446*, 1010−1016.

(17) Sharma, V.; Verma, V.; Lal, N.; Yadav, S. K.; Sarkar, S.; Mandalapu, D.; Porwal, K.; Rawat, T.; Maikhuri, J. P.; Rajender, S.; Sharma, V. L.; Gupta, G. Disulfiram and its novel derivative sensitize prostate cancer cells to the growth regulatory mechanisms of the cell by re-expressing the epigenetically repressed tumor suppressor—estrogen receptor β. *Mol. Carcinog.* **2016**, *55*, 1843−1857.

(18) Farooq, M. A.; Xu, L.; Aquib, M.; Ahsan, A.; Baig, M. M. F. A.; Wang, B. Denatured food protein-coated nanosuspension: A promising approach for anticancer delivery of hydrophobic drug. *J. Mol. Liq.* **2020**, *303*, 112690.

(19) Gu, J.; Su, Y.; Liu, P.; Li, P.; Yang, P. An environmentally benign antimicrobial coating based on a protein supramolecular assembly. *ACS Appl. Mater. Interfaces* **2017**, *9*, 198−210.

(20) Zhao, J.; Qu, Y.; Chen, H.; Xu, R.; Yu, Q.; Yang, P. Self-assembled proteinaceous wound dressings attenuate secondary trauma and improve wound healing in vivo. *J. Mater. Chem. B* **2018**, *6*, 4645−4655.

(21) Nasir, F.; Iqbal, Z.; Khan, J. A.; Khan, A.; Khuda, F.; Ahmad, L.; Khan, A.; Khan, A.; Dayoo, A.; Roohullah, fnm Development and evaluation of diclofenac sodium thermorevesible subcutaneous drug delivery system. *Int. J. Pharm.* **2012**, *439*, 120−126.

(22) Khan, S.; Minhas, M. U.; Ahmad, M.; Sohail, M. Self-assembled supramolecular thermoreversible β-cyclodextrin/ethylene glycol injectable hydrogels with difunctional Pluronic® 127 as controlled delivery depot of curcumin. Development, characterization and in vitro evaluation. *J. Biomater. Sci., Polym. Ed.* **2018**, *29*, 1−34.

(23) Cirillo, G.; Spataro, T.; Curcio, M.; Spizzirri, U. G.; Nicoletta, F. P.; Picci, N.; Iemma, F. Tunable thermo-responsive hydrogels: Synthesis, structural analysis and drug release studies. *Mater. Sci. Eng., C* **2015**, *48*, 499−510.

(24) Kim, Y.-J.; Matsunaga, Y. T. Thermo-responsive polymers and their application as smart biomaterials. *Mater. Sci. Eng., B* **2017**, *5*, 4307−4321.
(25) Liu, W.; Zhang, B.; Lu, W. W.; Li, X.; Zhu, D.; De Yao, K.; Wang, Q.; Zhao, C.; Wang, C. A rapid temperature-responsive sol−gel reversible poly (N-isopropylacrylamide)-g-methylcellulose copolymer hydrogel. *Biomaterials* **2004**, *25*, 3005−3012.
(26) Alinejad, Y.; Adoungotchodo, A.; Grant, M. P.; Epure, L. M.; Antoniou, J.; Mwale, F.; Lerouge, S. Injectable chitosan hydrogels with enhanced mechanical properties for nucleus pulposus regeneration. *Tissue Eng., Part A* **2019**, *25*, 303−313.
(27) Boisgard, A.-S.; Lamrayah, M.; Dzikowski, M.; Salmon, D.; Kirilov, P.; Primard, C.; Pirot, F.; Fromy, B.; Verrier, B. Innovative drug vehicle for local treatment of inflammatory skin diseases: Ex vivo and in vivo screening of five topical formulations containing poly (lactic acid)(PLA) nanoparticles. *Eur. J. Pharm. Biopharm.* **2017**, *116*, 51−60.
(28) Liu, L.; Tang, X.; Wang, Y.; Guo, S. Smart gelation of chitosan solution in the presence of NaHCO3 for injectable drug delivery system. *Int. J. Pharm.* **2011**, *414*, 6−15.
(29) Singh, A.; Narvi, S. S.; Dutta, P. K.; Pandey, N. D. External stimuli response on a novel chitosan hydrogel cross-linked with formaldehyde. *Biomater. Sci.* **2006**, *29*, 233−238.
(30) Sampath, U. G. T. M.; Ching, Y. C.; Chuah, C. H.; Singh, R.; Lin, P.-C. Preparation and characterization of nanocellulose reinforced semi-interpenetrating polymer network of chitosan hydrogel. *Cellulose* **2017**, *24*, 2215−2228.
(31) Liu, L.; Feng, X.; Pei, Y.; Wang, J.; Ding, J.; Chen, L. α-Cyclodextrin concentration-controlled thermo-sensitive supramolecular hydrogels. *Mater. Sci. Eng. Carbon* **2018**, *82*, 25−28.
(32) Zheng, Y.; Cheng, Y.; Chen, J.; Ding, J.; Li, M.; Li, C.; Wang, J.-c.; Chen, X. Injectable hydrogel−microsphere construct with sequential degradation for locally synergistic chemotherapy. *ACS Appl. Mater. Interfaces* **2017**, *9*, 3487−3496.
(33) Budianto, E.; Muthoharoh, S. P.; Nizardo, N. M. Effect of cross-linking agents, pH and temperature on swelling behavior of cross-linked chitosan hydrogel. *Asian J. Appl. Sci.* **2015**, *3*, 5.
(34) Ngah, W. W.; Hanafiah, M.; Yong, S. Adsorption of humic acid from aqueous solutions on cross-linked chitosan−epichlorohydrin beads: kinetics and isotherm studies. *Colloids Surf., B* **2008**, *65*, 18−24.
(35) Wang, S.-G.; Sun, X.-F.; Liu, X.-W.; Gong, W.-X.; Gao, B.-Y.; Bao, N. Chitosan hydrogel beads for fulvic acid adsorption: Behaviors and mechanisms. *Chem. Eng. J.* **2008**, *142*, 239−247.
(36) Yi, H.; Wu, L.-Q.; Bentley, W. E.; Ghodssi, R.; Rubloff, G. W.; Culver, J. N.; Payne, G. F. Biofabrication with chitosan. *Biomacromolecules* **2005**, *6*, 2881−2894.
(37) Dowding, P. J.; Vincent, B.; Williams, E. Preparation and swelling properties of poly (NIPAM)"minigel" particles prepared by inverse suspension polymerization. *J. Colloid Interface Sci.* **2000**, *221*, 268−272.
(38) Zhang, Y.; Wang, F.; Li, M.; Yu, Z.; Qi, R.; Ding, J.; Zhang, Z.; Chen, X. Self-Stabilized Hyaluronate Nanogel for Intracellular Codelivery of Doxorubicin and Cisplatin to Osteosarcoma. *Adv. Sci.* **2018**, *5*, 1700821.
(39) Zhang, Y.; Zhang, J.; Xu, W.; Xiao, G.; Ding, J.; Chen, X. Tumor microenvironment-labile polymer−doxorubicin conjugate thermogel combined with docetaxel for in situ synergistic chemotherapy of hepatoma. *Acta Biomater.* **2018**, *77*, 63−73.
(40) Chen, H.; Gu, Z.; An, H.; Chen, C.; Chen, J.; Cui, R.; Chen, S.; Chen, W.; Chen, X.; Chen, X.; Chen, Z.; Ding, B.; Dong, Q.; Fan, Q.; Fu, T.; Hou, D.; Jiang, Q.; Ke, H.; Jiang, X.; Liu, G.; Li, S.; Li, T.; Liu, Z.; Nie, G.; Ovais, M.; Pang, D.; Qiu, N.; Shen, Y.; Tian, H.; Wang, C.; Wang, H.; Wang, Z.; Xu, H.; Xu, J.-F.; Yang, X.; Zhu, S.; Zheng, X.; Zhang, X.; Zhao, Y.; Tan, W.; Zhang, X.; Zhao, Y. Precise nanomedicine for intelligent therapy of cancer. *Sci. China: Chem.* **2018**, *61*, 1503−1552.
(41) Zhang, L.; Tian, B.; Li, Y.; Lei, T.; Meng, J.; Yang, L.; Zhang, Y.; Chen, F.; Zhang, H.; Xu, H.; Zhang, Y.; Tang, X. A copper-mediated disulfiram-loaded pH-triggered PEG-shedding TAT peptide-modified lipid nanocapsules for use in tumor therapy. *ACS Appl. Mater. Interfaces* **2015**, *7*, 25147−25161.
(42) Huo, Q.; Zhu, J.; Niu, Y.; Shi, H.; Gong, Y.; Li, Y.; Song, H.; Liu, Y. pH-triggered surface charge-switchable polymer micelles for the co-delivery of paclitaxel/disulfiram and overcoming multidrug resistance in cancer. *Int. J. Nanomed.* **2017**, *12*, 8631.
(43) SARKAR, T.; AHMED, A. B. Development and in-vitro characterisation of chitosan loaded paclitaxel nanoparticle. *Asian J. Pharm. Clin. Res.* **2016**, *9*, 145−148.
(44) Liu, X.; Chu, H.; Cui, N.; Wang, T.; Dong, S.; Cui, S.; Dai, Y.; Wang, D. In vitro and in vivo evaluation of biotin-mediated PEGylated nanostructured lipid as carrier of disulfiram coupled with copper ion. *J. Drug Delivery Sci. Technol.* **2019**, *51*, 651−661.
(45) Cho, Y. I.; Park, S.; Jeong, S. Y.; Yoo, H. S. In vivo and in vitro anti-cancer activity of thermo-sensitive and photo-crosslinkable doxorubicin hydrogels composed of chitosan−doxorubicin conjugates. *Eur. J. Pharm. Biopharm.* **2009**, *73*, 59−65.
(46) Xu, Y.; Liu, Y.; Hu, X.; Qin, R.; Su, H.; Li, J.; Yang, P. The Synthesis of a 2D Ultra-Large Protein Supramolecular Nanofilm by Chemoselective Thiol−Disulfide Exchange and its Emergent Functions. *Angew. Chem., Int. Ed.* **2020**, *132*, 2872−2881.
(47) Ahsan, A.; Farooq, M. A. Therapeutic potential of green synthesized silver nanoparticles loaded PVA hydrogel patches for wound healing. *J. Drug Delivery Sci. Technol.* **2019**, *54*, 101308.
(48) Li, B.; Zhong, Q.; Li, D.; Xu, K.; Zhang, L.; Wang, J. Influence of ethylene glycol methacrylate to the hydration and transition behaviors of thermo-responsive interpenetrating polymeric network hydrogels. *Polymers* **2018**, *10*, 128.
(49) Choi, C.; Kim, S.; Pak, P.; Yoo, D.; Chung, Y. Effect of N-acylation on structure and properties of chitosan fibers. *Carbohydr. Polym.* **2007**, *68*, 122−127.
(50) Coelho, T. C.; Laus, R.; Mangrich, A. S.; de Fávere, V. T.; Laranjeira, M. C. M. Effect of heparin coating on epichlorohydrin cross-linked chitosan microspheres on the adsorption of copper (II) ions. *React. Funct. Polym.* **2007**, *67*, 468−475.
(51) Thürmer, M. B.; Diehl, C. E.; Brum, F. J. B.; Santos, L. A. d. Preparation and characterization of hydrogels with potential for use as biomaterials. *Mater. Res.* **2014**, *17*, 109−113.
(52) Guinesi, L. S.; Cavalheiro, É. T. G. The use of DSC curves to determine the acetylation degree of chitin/chitosan samples. *Thermochim. Acta* **2006**, *444*, 128−133.
(53) Kim, I. Y.; Yoo, M. K.; Seo, J. H.; Park, S. S.; Na, H. S.; Lee, H. C.; Kim, S. K.; Cho, C. S. Evaluation of semi-interpenetrating polymer networks composed of chitosan and poloxamer for wound dressing application. *Int. J. Pharm.* **2007**, *341*, 35−43.
(54) Nsereko, S.; Amiji, M. Localized delivery of paclitaxel in solid tumors from biodegradable chitin microparticle formulations. *Biomaterials* **2002**, *23*, 2723−2731.
(55) Fasehee, H.; Zarrinrad, G.; Tavangar, S. M.; Ghaffari, S. H.; Faghihi, S. The inhibitory effect of disulfiram encapsulated PLGA NPs on tumor growth: Different administration routes. *Mater. Sci. Eng. C* **2016**, *63*, 587−595.
(56) Jain, A.; Sharma, G.; Ghoshal, G.; Kesharwani, P.; Singh, B.; Shivhare, U. S.; Katare, O. P. Lycopene loaded whey protein isolate nanoparticles: An innovative endeavor for enhanced bioavailability of lycopene and anti-cancer activity. *Int. J. Pharm.* **2018**, *546*, 97−105.
(57) Prusty, A.; Parida, P. Development and Evaluation of gel incorporated with biogenically synthesized silver nanoparticles. *J. Appl. Biopharm. Pharmacokinet.* **2014**, *3*, 1−6.
(58) Ahmad, U.; Sohail, M.; Ahmad, M.; Minhas, M. U.; Khan, S.; Hussain, Z.; Kousar, M.; Mohsin, S.; Abbasi, M.; Shah, S. A.; Rashid, H. Chitosan based thermosensitive injectable hydrogels for controlled delivery of loxoprofen: development, characterization and in-vivo evaluation. *Int. J. Biol. Macromol.* **2019**, *129*, 233−245.
(59) Kocak, F. Z.; Talari, A. C. S.; Yar, M.; Rehman, I. U. In-Situ Forming pH and Thermosensitive Injectable Hydrogels to Stimulate Angiogenesis: Potential Candidates for Fast Bone Regeneration Applications. *Int. J. Mol. Sci.* **2020**, *21*, 1633.

https://dx.doi.org/10.1021/acsomega.0c02548
ACS Omega 2020, 5, 20450−20460

(60) Rehmani, S.; Ahmad, M.; Minhas, M. U.; Anwar, H.; Zangi, M. I.-u. -d.; Sohail, M. Development of natural and synthetic polymer-based semi-interpenetrating polymer network for controlled drug delivery: optimization and in vitro evaluation studies. *Polym. Bull.* **2017**, *74*, 737−761.

https://dx.doi.org/10.1021/acsomega.0c02548
ACS Omega 2020, 5, 20450−20460